Ghost interference in double-slit experiment with type-II parametric down-conversion resource

Mingyang Zheng (郑名扬)[1,2], Lian Chen (陈 炼)[1,2], Xindong Cai (蔡昕东)[2,3], and Ge Jin (金 革)[1,2*]

[1] *State Key Laboratory of Particle Detection and Electronics, University of Science and Technology of China, Hefei 230026, China*

[2] *Department of Modern Physics, University of Science and Technology of China, Hefei 230026, China*

[3] *Hefei National Laboratory for Physical Sciences at Micro Scale, University of Science and Technology of China, Hefei 230026, China*

[*] *Corresponding author: goldjin@ustc.edu.cn*

Received February 5, 2013; accepted March 28, 2013; posted online May 30, 2013

A double-slit ghost interference experiment performed on an entangled resource using type-II non-collinear degenerate spontaneous parametric down-conversion (SPDC) is demonstrated. The influence of the distance between the double-slit and the bucket detector preceded by a pinhole is studied. The experimental results show that the interference fringes become increasingly distinct with higher visibility when the pinhole-double-slit distance increases. A first-order classical theory based on the Klyshko's two-photon advanced-wave picture, and a second-order quantum-image theory are provided for explanations. The fitting results indicate that the divergence of the converted fluorescence significantly affects the ghost fringes.

OCIS codes: 190.0190, 270.0270.
doi: 10.3788/COL201311.071901.

During the past few decades, the correlated properties of entangled two-photon states have attracted much attention due to its extensive application on quantum optics and information[1,2]. Spontaneous parametric down-conversion(SPDC), a common method of producing entangled photons, could generate correlated photons with energy and momentum conserved, which are conventionally called signal and idler beam[3−6]. Using the transverse spatial correlation of biphotons, the 'ghost' image of an object could be drawn in the path without the object via coincidence measurement between the bucket detection in the signal beam and the transverse scanning in the idler beam. The ghost Young's interference experiments[7,8], first demonstrated in the mid 1990's, has inspired much research in the following years[9]. Barbosa *et al.*[10,11] found that the visibility of the ghost interference pattern was related to the signal pinhole dimension; hence, they developed a quantum theory to provide some interpretations. The spatial correlations of the entangled photon pairs could be controlled by the angular spectrum of the pump beam[12], and could capture the image of a nonlocal double-slit in ghost configuration[13]. Ghost interference can provide experimental verifications for certain quantum theories[14,15], and has also inspired several practical applications, such as quantum cryptography[16], quantum metrology[17], and quantum lithography[18,19]. The argument on whether or not the entanglement property is decisive in ghost experiments lasted a long time until it was realized with pseudothermal light[20−25].

In this letter, the ghost interference experiment is performed on an entangled resource. The schematic of the experimental setup is shown in Fig. 1. A 405-nm semiconductor CW laser is used to pump a 2-mm-long beta barium borate (BBO) crystal cut for type-II non-collinear degenerate SPDC (shown in Fig. 2). The pump laser photon, with frequency $\omega_{\rm p}$ and wave vector $\mathbf{k}_{\rm p}$, is converted into signal $(\omega_{\rm s}, \mathbf{k}_{\rm s})$ and idler $(\omega_{\rm i}, \mathbf{k}_{\rm i})$ photons with $\omega_{\rm s} = \omega_{\rm i} = \omega_{\rm p}/2$ and $\mathbf{k}_{\rm p} = \mathbf{k}_{\rm s} + \mathbf{k}_{\rm i}$. A pump beam orientation of $\Theta_{\rm p} = 42.2°$, with respect to the optical axis, simulates the conversion crystal with down converted pairs of orthogonally polarized signal and idler photons centered at $\lambda = 810$ nm and propagate freely in two cones intersecting in $\mathbf{k}_{\rm p}$'s vertical plane, resulting in an angle of $\phi_{\rm s,i} = 3°$ with respect to the pump beam as shown in Fig. 2. The transmitted laser photons are collected by a light trash can to decrease accidental coincidences.

The signal beam travels about 30 cm to pass through a double-slit, and then propagates freely to the detection system. In the detection system, the signal photons pass through a pinhole with a diameter of $h = 0.3$ mm, a 810-nm spectral filter F_1 with 11-nm FWHM bandwidth, and are then coupled into a multimode fiber connected

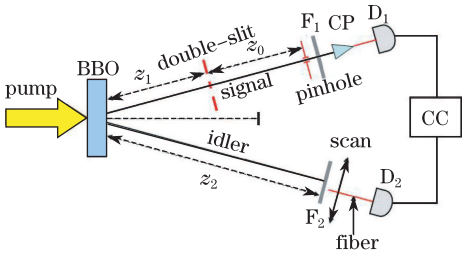

Fig. 1. (Color online) Schematic of the experimental setup. Ghost interference is observed by transverse scanning of the fiber tip in the idler path, with coincidence measurement in a 2.4-ns coincidence time window. The double-slit in the signal beam has a width of $a = 0.15$ mm and a slit distance of $d = 0.45$ mm. The relevant distances in the experiment are $z_1 = 30$ cm and $z_2 = 61$ cm, while z_0 is a variable. $F_{1,2}$ and $D_{1,2}$ are the filters and detectors, respectively. CP is a coupler.

with an avalanche photo diode (APD). In the idler path, the beam travels a distance of about 61 cm from the crystal to the input end of another multimode optical fiber whose output end is coupled to an APD detector. The fiber tip is scanned transversely by an encoder driver. In front of the scanning fiber, a spectra filter F_2, centered at 810 nm with 20-nm bandwidth, is inserted.

The experimental results are presented in Fig. 3 showing the influence of the distance between the double-slit and the pinhole on the interference fringes. The interference pattern is observed by recording the coincidence counts as a function of the transverse position in the scanning plane. A series of distances is chosen: $z_0 = 10$, 20, 50, and 80 cm. The ghost interference pattern is a typical Young's interference shape fitted with the first-order coherence theory presented in Ref. [7]. The period of the interference oscillation is determined by the distances between the crystal to the slits in the signal beam z_1 and the crystal to the idler detector z_2. With the increase of the pinhole-double-slit distance, the interference pattern becomes increasingly distinct with higher visibility, as is shown in Fig. 3. Both a classical first-order theory and a second-order theory are presented to provide some explanations.

Figure 4 shows the Klyshko's advanced-wave picture[26,27]. In this simple model, using transverse momentum conservation and geometry configuration,

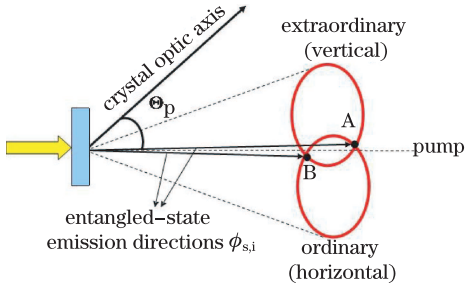

Fig. 2. (Color online) Non-collinear degenerate type-II SPDC cones. Correlated photons, one for e-polarization and the other for o-polarization, lie on the opposite sides of the pump beam. The photons in the intersections (A, B) of the cones are entangled: $(|\mathrm{H}\rangle_\mathrm{A}|\mathrm{V}\rangle_\mathrm{B} + \mathrm{e}^{\mathrm{i}\alpha}|\mathrm{V}\rangle_\mathrm{A}|\mathrm{H}\rangle_\mathrm{B})/\sqrt{2}$, where α is the phase difference.

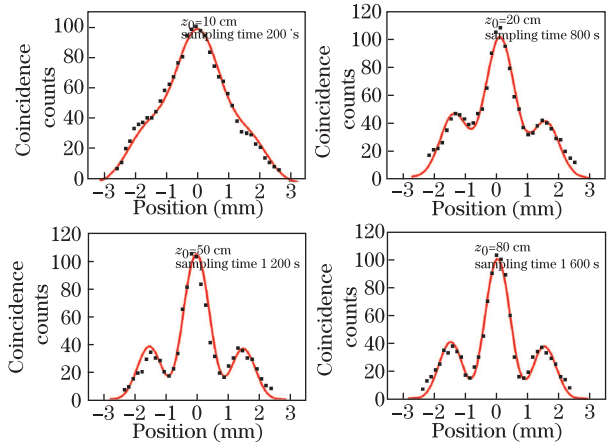

Fig. 3. (Color online) The two-photon double-slit "ghost" interference pattern for different distances between the object and the pinhole.

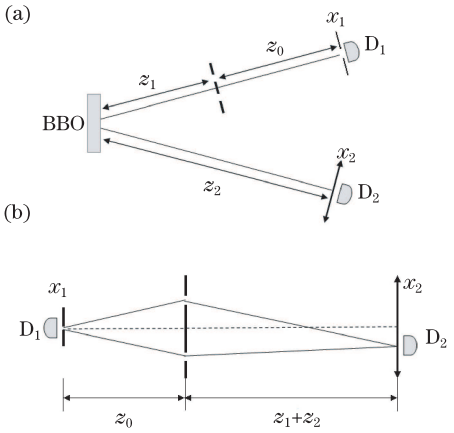

Fig. 4. (Color online) Demonstration of the Klyshko's advanced-wave picture. (a) Simplified experimental scheme; (b) first-order picture.

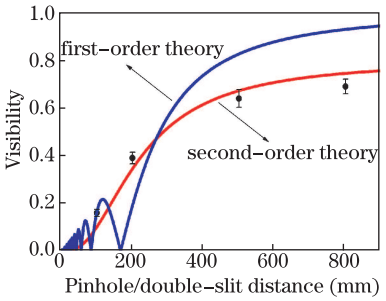

Fig. 5. (Color online) Visibility versus the pinhole/double-slit distance fitting with the first-order and second-order theories.

the pinhole plays the role of ghost source and the BBO crystal serves as a mirror for reflecting the interference fringe in the idler observation screen. In this study, a classical first-order theory developed to describe the variation of visibility in the experiment. In this model, the ghost source is considered to be an evenly distributed light field and treated as a constant in the transverse plane. The visibility of the two-photon interference pattern versus the pinhole-double-slit distance could then be described as

$$u_1 = \frac{\sin(\pi h d/\lambda z_0)}{\pi h d/\lambda z_0}. \tag{1}$$

The simulated result is displayed in Fig. 5. The experimental results can be approximately explained, but the exact prediction is inaccessible because the momentum-momentum correlation of the signal-idler pairs is perfect in Klyshko's picture, and the replacement of the crystal by a mirror is allowed. However, in actual situation, the momentum-momentum correlation is imperfect.

For a precise interpretation, a second-order quantum-image theory, considering the pump width and divergence, is needed. In the multimode monochromatic theory[11], the divergence of the wave vector in the signal beam $\mathbf{k}_\mathrm{s}$ and idler beam $\mathbf{k}_\mathrm{i}$ has been considered. This theory demonstrates that the divergence of the biphoton wave vector is responsible for the interference visibility, and an extremely high visibility could be achieved when the divergence is infinitesimal. The dependence of the

visibility on the pinhole-double-slit distance could be expressed by

$$u_2 = u_0\Big(\frac{4z_0}{ahk}\Big)^2\big[-2{}_2F_1(D)+{}_2F_1(D_+)+{}_2F_1(D_-)\big], \tag{2}$$

where u_0 is a constant, k is the wave number of the down-converted photons, and ${}_2F_1$ is the hypergeometric function.

$$D = \Big\{-\frac{1}{2},\frac{1}{2},\frac{1}{2},-\Big(\frac{dhk}{4z_0}\Big)^2\Big\}, \tag{3}$$

$$D_+ = \Big\{-\frac{1}{2},\frac{1}{2},\frac{1}{2},-\Big[\frac{(2d+a)hk}{8z_0}\Big]^2\Big\}, \tag{4}$$

$$D_- = \Big\{-\frac{1}{2},\frac{1}{2},\frac{1}{2},-\Big[\frac{(2d-a)hk}{8z_0}\Big]^2\Big\}. \tag{5}$$

The second-order result is shown in Fig. 5. The quantum theory provides a better explanation, and it can predict the experimental results. The fitting results indicate that the divergence of the converted fluorescence significantly affects the ghost fringes.

In conclusion, a ghost interference experiment is carried out on an entangled resource. This study focuses on the influence of the distance between the object and the pinhole on the interference pattern. With the increase in distance, the quality of the interference pattern becomes better with high visibility. The classical first-order theory based on the Klyshko's advanced-wave picture, and a quantum multimode monochromatic theory, are developed to explain the experimental results. The fitting results indicate that the classical first-order theory can provide a qualitative physics picture, while the quantum-image theory can present a quantitative data of the visibility.

The authors would like to thank Prof. Jianwei Pan and Prof. Chao Zhai for providing the equipment for the experiment. This work was supported by the National Natural Science Foundation of China under Grant No. 11075152.

References

1. T. B. Pittman, Y. H. Shih, D. V. Strekalov, and A. V. Sergienko, Phys. Rev. A **52,** R3429 (1995).
2. A. K. Ekert, Phys. Rev. Lett. **67,** 661 (1991).
3. P. G. Kwiat, K. Mattle, H. Weinfurter, A. Zeilinger, A. V. Sergienko, and Y. H. Shih, Phys. Rev. Lett. **75,** 4337 (1995).
4. S. P. Walborn and C. H. Monken, Phys. Rev. A **76,** 062305 (2007).
5. M. D'Angelo, Y. H. Kim, S. P. Kulik, and Y. H. Shih, Phys. Rev. Lett. **92,** 233601 (2004).
6. G. Scarcelli, Y. Zhou, and Y. H. Shih, Eur. Phys. J. D **44,** 167 (2007).
7. P. H. S. Ribeiro, S. Pádua, J. C. M. da Silva, and G. A. Barbosa, Phys. Rev. A **49,** 4176 (1994).
8. D. V. Strekalov, A. V. Sergienko, D. N. Klyshko, and Y. H. Shih, Phys. Rev. Lett. **74,** 3600 (1995).
9. S. P. Walborn, C. H. Monken, S. Pádua, and P. H. S. Ribeiro, Phys. Rep. **495,** 87 (2010).
10. P. H. S. Ribeiro and G. A. Barbosa, Phys. Rev. A **54,** 3489 (1996).
11. G. A. Barbosa, Phys. Rev. A **54,** 4473 (1996).
12. C. H. Monken, P. H. S. Ribeiro, and S. Pádua, Phys. Rev. A **57,** 3123 (1998).
13. E. J. S. Fonseca, P. H. S. Ribeiro, S. Pádua, and C. H. Monken, Phys. Rev. A **60,** 1530 (1999).
14. A. Einstein, B. Podolsky, and N. Rosen, Phys. Rev. **35,** 777 (1935).
15. Y. H. Kim and Y. H. Shih, Found. Phys. **29,** 1849 (1999).
16. C. Bennett, F. Bessette, G. Brassard, L. Salvail, and J. Smolin, J. Cryptology **5,** 3 (1992).
17. A. Migdall, Phys. Today **52,** 41 (1999).
18. A. N. Boto, P. Kok, D. S. Abrams, S. L. Braunstein, C. P. Williams, and J. P. Dowling, Phys. Rev. Lett. **85,** 2733 (2000).
19. M. D'Angelo, M. V. Chekhova, and Y. H. Shih, Phys. Rev. Lett. **87**, 013602 (2001).
20. R. S. Bennink, S. J. Bentley, R. W. Boyd, and J. C. Howell, Phys. Rev. Lett. **92,** 033601 (2004).
21. J. Cheng and S. S. Han, Phys. Rev. Lett. **92,** 093903 (2004).
22. D. Duan and Y. Xia, Chin. Opt. Lett. **10,** 031102 (2012).
23. F. Ferri, D. Magatti, A. Gatti, M. Bache, E. Brambilla, and L. A. Lugiato, Phys. Rev. Lett. **94,** 183602 (2005).
24. A. Valencia, G. Scarcelli, M. D'Angelo, and Y. H. Shih, Phys. Rev. Lett. **94,** 063601 (2005).
25. B. Cao, C. Zhang, and P. Ou, Chin. Opt. Lett. **9,** 081102 (2011).
26. D. N. Klyshko, Phys. Lett. A **132,** 299 (1988).
27. A. V. Belinskii and D. N. Klyshko, JETP **78,** 259 (1994).